

Phase coexistence and magnetocaloric effect in $\text{La}_{5/8-y}\text{Pr}_y\text{Ca}_{3/8}\text{MnO}_3$ ($y=0.275$)

M. H. Phan,^{*†} M. B. Morales, N. S. Bingham, and H. Srikanth^{*‡}

Department of Physics, University of South Florida, Tampa, Florida 33620, USA

C. L. Zhang and S. W. Cheong

Rutgers Center for Emergent Materials and Department of Physics & Astronomy, Rutgers University, Piscataway, New Jersey 08854, USA

(Received 4 March 2009; revised manuscript received 9 February 2010; published 12 March 2010)

The magnetocaloric effect (MCE) was measured to probe the nature of phase coexistence of structurally different ferromagnetic metallic (FMM) and charge-ordered insulating phases in $\text{La}_{5/8-y}\text{Pr}_y\text{Ca}_{3/8}\text{MnO}_3$ ($y=0.275$) single crystals. The MCE peaks with both positive and negative values are observed in the vicinity of the multiple-phase transitions in the system. Strain associated with the phase coexistence has been known to stabilize a strain-glass state as well as a strain-liquid state. The large MCE is observed in the “dynamic” strain liquid state, while it is relatively small in the “frozen” strain-glass state. The MCE data reveal that the sharp increase in the magnetization below the Curie temperature in the strain-liquid region is attributed to the enhancement of the FM domain regions that are already present in the material. MCE is also shown to be a useful method to probe the subtle balance of coexisting phases in mixed-phase manganites.

DOI: 10.1103/PhysRevB.81.094413

PACS number(s): 75.30.Kz, 75.30.Sg

I. INTRODUCTION

Mixed-phase manganites of $R_{1-x}M_x\text{MnO}_3$ ($R=\text{La}, \text{Pr}, \text{Nd}$, and Sm and $M=\text{Sr}, \text{Ca}, \text{Ba}$, and Pb) exhibit rich variety in terms of coexisting and competing magnetic and electronic phases.^{1,2} Of particular interest is the charge-ordered insulating (COI) phase that coexists and strongly competes with the ferromagnetic metallic (FMM) phase and is unstable under various perturbations such as carrier doping, strain, magnetic field, electric field, and current.^{3–17} CO occurs in a material when the long-range Coulomb interaction, among the carriers, overcomes their kinetic energy.³ CO has been widely observed in manganites possessing narrow one-electron bandwidth (W), such as $\text{Pr}_{1-x}\text{Ca}_x\text{MnO}_3$ ($0.3 \leq x \leq 0.5$) and $\text{Nd}_{1-x}\text{Ca}_x\text{MnO}_3$ ($0.4 \leq x \leq 0.5$) compounds.^{4,5} In these compounds, the double-exchange interaction is suppressed and hence the pseudotetragonal CO phase has a comparable free energy to the pseudocubic FM phase, leading to an intrinsic phase separation.¹ However, the physical origin of the phase separation in some of the mixed-phase manganites such as $\text{La}_{5/8-y}\text{Pr}_y\text{Ca}_{3/8}\text{MnO}_3$ (LPCMO) is not fully understood in part due to the complex nature of the system.^{6–17} LPCMO is a mixture of $\text{La}_{5/8}\text{Ca}_{3/8}\text{MnO}_3$ ($y=0$) and $\text{Pr}_{5/8}\text{Ca}_{3/8}\text{MnO}_3$ ($y=5/8$) exhibiting low-temperature FMM and COI ground states, respectively. In this system, the substitution of smaller Pr ions for larger La ions reduces W , thus leading to micrometer scale phase separation with multiple phases coexisting in the material.^{6,7} It has been argued that in the presence of quenched disorder induced by the ions of different radii, the similarity of the free energies lead to the coexistence of the competing FMM and COI phases.¹⁸ If this is the case, the phase separation should be static because the phase boundaries are pinned by the disorder sites. However, experimental studies have revealed that these phase boundaries are not fully pinned in LPCMO (Refs. 6, 8, 10, 11, 15, and 16) and hence the inherent coexistence of the FMM and COI phases at the micron length scale is inconsistent with the notion of a charge-segregation type of phase separation.^{1,2,19}

It has been suggested that the different crystal structures of the FMM and COI phases generate long-range strain interactions leading to an intrinsic variation in elastic energy landscape, which in turn leads to phase separation (PS) into the strain-liquid and strain-glass regimes.^{6,12,15} It has also been suggested that phase separated regions strongly interact with each other via martensitic accommodation strain which leads to a cooperative freezing of the combined charge/spin/strain degrees of freedom.^{11,16} As a result, LPCMO undergoes a transition from the strain-liquid state to the strain-glass state. Since the strain-liquid state shows large fluctuations in resistivity^{6,11} and can easily be transformed into a metallic state by applying an external electric field,¹⁵ it is considered as a “dynamic” PS. In contrast, effect of electric field is negligible on the frozen strain-glass state thus classifying it as a “static” PS.¹⁵ A notable feature is that unlike the case of a canonical spin-glass phase, in the strain-glass phase the FMM volume fraction of LPCMO varies remarkably, contributing to the magnetic relaxation as the glass transition is crossed.^{10,13} Despite a number of previous works,^{9,11,12} the effect of magnetic field on the strain-liquid and strain-glass states has not been studied in detail. Another emerging issue, still under debate, is the underlying origin of the sharp increase in the magnetization below the Curie temperature (T_C) in the strain-liquid region. Two different mechanisms have been proposed for interpreting this observation.^{8,11,12,15,17} In the first scenario, it is proposed that with lowering temperature, the COI state is spontaneously destabilized to the FMM phase giving rise to a coexistence of these two phases, and the sharp increase of the magnetization below T_C is due to the melting of the COI state.^{11,12} This is similar to the case of charge-ordered $R_{0.5}\text{Sr}_{0.5}\text{MnO}_3$ ($R=\text{La}, \text{Pr}$, and Nd) manganites.^{1,3,20} In the second scenario, it has been suggested that the increase in magnetization occurs via the growth of FMM domain regions that are already present in the material even in zero magnetic field.^{8,15,17}

To shed light on these important unresolved issues, it is essential to employ experimental methods that allow detailed

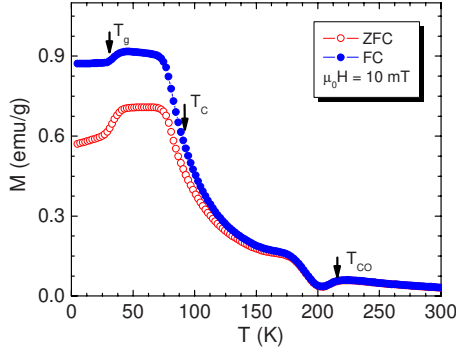


FIG. 1. (Color online) Temperature dependence of ZFC and FC magnetization taken at $\mu_0 H = 10$ mT for LPCMO.

investigations of the temperature and magnetic field responses of the different phases. In this study, we introduce magnetocaloric effect (MCE) experiments as being ideally suited for this purpose. While MCE is generally considered in the community as an “applied” measurement tool to characterize magnetic refrigerant materials,²¹ we demonstrate that it is actually a very useful probe of magnetic transitions and ground-state magnetic properties in mixed-valent manganites like the $\text{La}_{5/8-y}\text{Pr}_y\text{Ca}_{3/8}\text{MnO}_3$ ($y=0.275$) system.

II. RESULTS AND DISCUSSION

Single crystals of $\text{La}_{5/8-y}\text{Pr}_y\text{Ca}_{3/8}\text{MnO}_3$ ($y=0.275$) samples (LPCMO) were grown in an optical floating-zone furnace.^{7,10} X-ray diffraction confirmed the phase purity of the crystals. Magnetic and magnetocaloric measurements were performed using a physical property measurement system from Quantum Design in the temperature range of 5–300 K at applied fields up to 7 T.

Figure 1 shows the zero-field-cooled (ZFC) and field-cooled (FC) magnetization curves taken at 10 mT applied field with the data recorded while warming up. It is observed that the LPCMO system undergoes multiple magnetic transitions. A peak at $T_{\text{CO}} \sim 205$ K is due to the COI transition,¹¹ and a shoulder at a lower temperature of about 175 K arises from antiferromagnetic (AFM) ordering.¹² As T is further decreased, the magnetization sharply increases and an FMM transition is observed at $T_c \sim 90$ K on warming (~ 75 K on cooling). A drop in magnetization is observed at $T_g \sim 30$ K, below which the system enters the frozen strain-glass state from the dynamic strain-liquid state.^{11–13,16} It has been shown that T_g is actually the re-entrant COI transition temperature.^{11,16} These multiple features will be probed and analyzed using MCE experiments, as discussed below.

To evaluate the MCE of a magnetic material, the magnetic-entropy change (ΔS_M) is often calculated from a family of isothermal M - H curves using the Maxwell relation,²¹

$$\Delta S_M = \mu_0 \int_0^{H_{\max}} \left(\frac{\partial M}{\partial T} \right)_H dH, \quad (1)$$

where M is the magnetization, H is the magnetic field, and T is the temperature. From Eq. (1), we note that $\Delta S_M(T)$ is

directly related to the first derivative of magnetization with respect to temperature ($\partial M / \partial T$) and so the MCE is expected to be inherently more sensitive for probing magnetic transitions than conventional magnetization and resistivity measurements. Importantly, the sign of ΔS_M , which is determined by the slope change of the dM/dT curve, can allow probing the magnetic transitions further to better understand the nature of the different phases in a material with a rich and complex H - T magnetic phase diagram.^{22–24} Following the convention in MCE analysis, the value of $-\Delta S_M$ is *positive* for materials exhibiting an FM transition, because of the fully magnetically ordered configuration with the application of an external magnetic field.^{21,25} The *negative* values of $-\Delta S_M$ are associated with AFM ordering in systems due to orientational disorder of the magnetic sublattice antiparallel to the applied magnetic field.^{23,26} Recently, von Ranke *et al.*²⁷ have theoretically investigated the implications of positive and negative MCEs in antiferromagnetic and ferromagnetic spin configurations.

It has been noted that the influence of magnetic irreversibility (e.g., large field hysteresis) on the estimation of the MCE [i.e., the peak magnitude of $\Delta S_M(T)$] from the isothermal M - H curves using Maxwell equation could result in ambiguous values for some first-order magnetic transition materials^{28–31} if the M - H measurements are not conducted in an equilibrium regime.³² In the equilibrium regime, the M - H curves measured with increasing and decreasing magnetic fields should coincide with each other (i.e., zero or negligible field hysteresis), and the validation of Maxwell equation for calculating the magnetic-entropy change has been established.³² For the case of LPCMO, we recall that large magnetic irreversibility appears to occur just below T_{CO} , due to the coexistence of the FMM and COI phases. Therefore, we measured the M - H curves using the following measurement protocol to eliminate any influence from the hysteresis. Before conducting any M - H measurements at temperatures below T_{CO} , the sample was cooled in zero magnetic field from above T_{CO} . At each temperature, the magnetization was measured as the magnetic field was continuously swept from 0 to 6 T (labeled the virgin M - H curve); then from 6 T to 0 (labeled the return M - H curve); and finally from 0 to 6 T (labeled the second M - H curve). The M - H data were taken first at 300 K and subsequently at lower temperatures following the same measurement protocol. Figure 2 shows the M - H data at selected temperatures with the “virgin,” “return,” and “second” curves labeled. These data clearly indicate large field hysteresis in LPCMO. It is worth noting that for $T > 75$ K, a reversible magnetization is observed as the applied magnetic field is cycled (i.e., the second M - H curves coincide with the virgin M - H curves). However, for $T < 75$ K the second M - H curves do not coincide with the virgin M - H curves but coincide with the return M - H curves below 65 K. The same state is observed as the applied magnetic field is continued to be cycled up and down further.

To capture these intriguing features from the perspective of MCE, we have calculated the magnetic-entropy change from the M - H curves *taken after completing one cycle of applied field* (i.e., the second M - H curves). This helps avoid the hysteresis problem in calculating the magnetic-entropy change of LPCMO using Eq. (1). Figure 3 shows the tem-

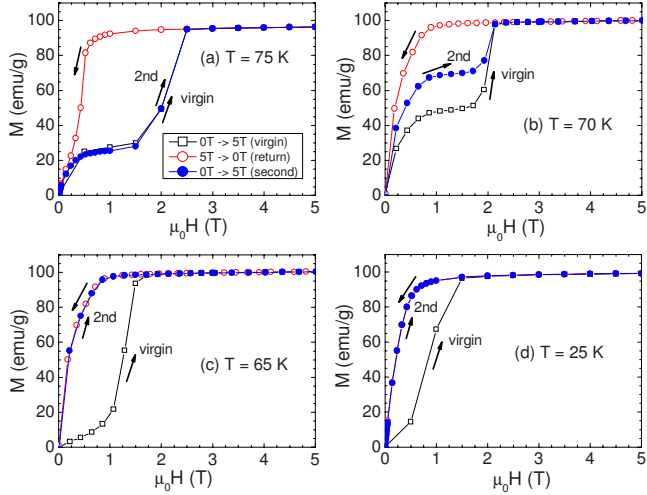


FIG. 2. (Color online) The M - H curves for some selected temperatures (a) $T=75$ K, (b) $T=70$ K, (c) $T=65$ K, and (d) $T=25$ K. The arrows indicate the way in which the virgin, return, and second magnetization curves were measured.

perature dependence of $-\Delta S_M$ for the magnetic field change of 1.5 T and 6 T, respectively. As expected, $-\Delta S_M(T)$ curves exhibit peaks around T_{CO} , T_C , and T_g . The positive values of $-\Delta S_M$ around T_C and the negative values of $-\Delta S_M$ around T_{CO} and T_g (at low applied fields, $\Delta\mu_0H < 2$ T) are consistent with the LPCMO undergoing the ferromagnetic, charge ordering and re-entrant charge-ordering transitions, respectively. We recall that in charge-ordered $R_{0.5}Sr_{0.5}MnO_3$ ($R=Pr$ and Nd) systems,^{26,31} the COI phase is the low-temperature phase and the FMM phase is the high-temperature phase. In that case, entropy is smaller in the COI phase than in the FMM phase, so the application of a magnetic field lowers the transition temperature and leads to the negative value of $-\Delta S_M$. However, the opposite situation is observed for LPCMO, which exhibits the FMM and COI states as the ground and high-temperature states, respectively. Since entropy is smaller in the FMM phase than in the COI phase, the positive value of $-\Delta S_M$ is obtained at the T_C . Such a difference in sign of $-\Delta S_M$ distinguishes the ground-state magnetic properties of LPCMO from those of the $R_{0.5}Sr_{0.5}MnO_3$ ($R=Pr$ and Nd) systems.^{26,31}

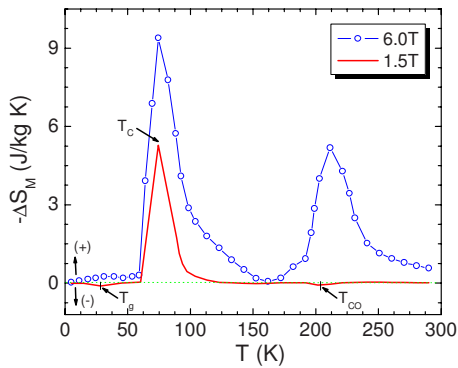


FIG. 3. (Color online) Temperature dependence of magnetic-entropy change ($-\Delta S_M$) for LPCMO for the magnetic field change of 1.5 T and 6 T, respectively.

It is noted in Fig. 3 that the $-\Delta S_M$ has the largest variation at $T \sim 75$ K (in the dynamic SP state), while it is comparatively very small at temperatures $\sim T_g$ (in the frozen SP state). This indicates that the strain-liquid state is strongly affected by an applied magnetic field, whereas the strain-glass state is relatively magnetic field independent. This may also be reconciled with the analogous observation that an electric field significantly affects the dynamic PS state but has a negligible effect on the frozen PS state.¹⁵ Our finding also points to the important fact that for $T < T_C$, the dynamics of the AFM to FM transition is kinetically arrested and as a result, in zero applied magnetic field, the material cannot fully reach its preferred ground state which is ferromagnetic.³³ In the strain-liquid region, the large variation of $-\Delta S_M$ (Fig. 3) is attributed to the suppression of dynamic fluctuations (dynamic phase separation) in magnetic fields. The largest value of $-\Delta S_M$ at ~ 75 K is likely the result of the strongest dynamic fluctuation and coincides with the drop in electrical resistivity that occurs at this temperature.^{11,12} The large variation of $-\Delta S_M$ in the dynamic PS region (Fig. 3) can also be correlated with the strong increase in the magnetization below T_C (Fig. 1). The shape of $-\Delta S_M(T)$ curves observed at T_C for LPCMO is quite similar to that observed for RCO_2 ($R=Dy$, Ho, and Er) systems,³⁴ which showed a sharp jump in $-\Delta S_M$ around the magnetic-ordering temperature, with a good agreement between the experimental data and theoretical calculations. Nevertheless, we would like to clarify about the presence of a ΔS_M spike in some mixed-phase materials such as $La_{0.7}Pr_{0.3}Fe_{11.5}Si_{1.5}$,³⁰ where paramagnetic and ferromagnetic phases coexist in the vicinity of the Curie temperature. In those cases, the field-induced metamagnetic transition takes place in the paramagnetic phase and so the low-field magnetization change does not contribute to the ΔS_M .³⁰ However, the case is different for LPCMO, where the contribution to the ΔS_M results from the low-field magnetization change in the ferromagnetic phase and the high-field magnetization change related to the fact that the field-induced metamagnetic transition takes place in the antiferromagnetic phase. In addition, the M - H curves on our system have been measured for LPCMO in the equilibrium regime. Therefore, the spike feature in ΔS_M is ruled out in this case and as a cautionary note, one has to be careful with the MCE experimentation and analysis of mixed-phase materials.

To clarify if the strong increase in the magnetization below T_C is attributed to the destabilization of the COI phase^{11,12} or due to the enhancement of pre-existing FMM domains in the material,^{8,15,17} we plot in Fig. 4 the magnetic field dependencies of the maximum magnetic-entropy change ($-\Delta S_M^{\max}$) and the magnetization (M) at 75 K. It is observed in Fig. 4(a) that the $-\Delta S_M^{\max}$ increases rapidly and quite linearly with increasing H up to 2.6 T and then remains almost constant for $H > 2.6$ T. This dependence of $-\Delta S_M^{\max}(H)$ can be correlated with the $M(H)$ dependence. We note that at 75 K the COI and FMM phases coexist and both of them are magnetic field dependent. The change in the FMM phase can be achieved at a lower magnetic field while a higher magnetic field is needed to change the COI phase. As extracted from the M - H curve [Fig. 4(b)], $H_{S1}=1.5$ T is a critical magnetic field at which the COI phase starts to

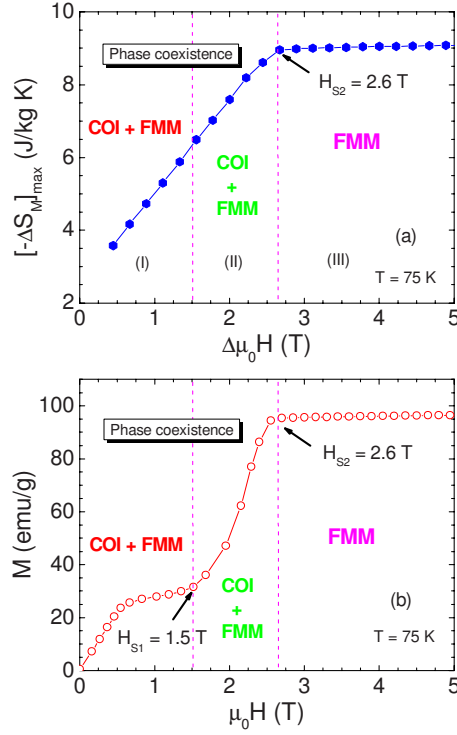


FIG. 4. (Color online) (a) Magnetic field dependence of maximum magnetic-entropy change ($-\Delta S_M^{\max}$) for LPCMO at 75 K; (b) the magnetic hysteresis loop $M(H)$ at 75 K. $H_{S1}=1.5$ T—the critical magnetic field at which the COI phase starts to convert into the FMM phase; $H_{S2}=2.6$ T—the critical magnetic field at which the COI phase converts fully into the FMM phase. The coexistence of the COI and FMM phases is below $H_{S2}=2.6$ T.

convert into the FMM phase while $H_{S2}=2.6$ T is a critical magnetic field at which the COI phase converts fully into the FMM phase. Therefore it can be concluded that for $H < H_{S1}$ the $-\Delta S_M^{\max}$ results solely from the variation of the magnetization in the FMM phase, since the applied magnetic field has a negligible effect on the COI phase. For $H_{S1} < H < H_{S2}$, however, the COI phase converts into the FMM phase thus also contributing to $-\Delta S_M^{\max}$. For $H > H_{S2}$, the constancy of $-\Delta S_M^{\max}$ can be attributed to the complete conversion of the COI phase into the FMM phase. According to this, it is quite natural to infer, at first glance, that the sharp increase of the magnetization below T_C for LPCMO is due to the destabilization of the COI phase,^{11,12} similar to the cases reported in the charge-ordered $R_{0.5}\text{Sr}_{0.5}\text{MnO}_3$ ($R=\text{Pr}$ and Nd) manganites.^{26,31} However, we note that a critical magnetic field needed to fully convert COI into FMM is often very high for charge-ordered manganites [for example, at ~ 75 K, $H_{S2} \sim 12$ T for $\text{La}_{1-x}\text{Ca}_x\text{MnO}_3$ ($x=0.5$) (Ref. 17) and $H_{S2} \sim 8-17$ T for $\text{Pr}_{1-x}\text{Ca}_x\text{MnO}_3$ ($0.3 \leq x \leq 0.5$) (Ref. 4)]. For the case of LPCMO, the volume fraction of the COI phase at 75 K is large $\sim 69\%$ (determined from the $M-H$ curve in Fig. 4(b) using the same method employed in Ref. 8) and the application of a magnetic field ~ 2.6 T is unlikely to be strong enough to convert COI fully into FMM. This can also be reconciled with the fact that at 75 K the $-\Delta S_M^{\max}$ resulting from the variation of the magnetization in the FM phase (~ 6.49 J/kg K) is about twice larger than that result-

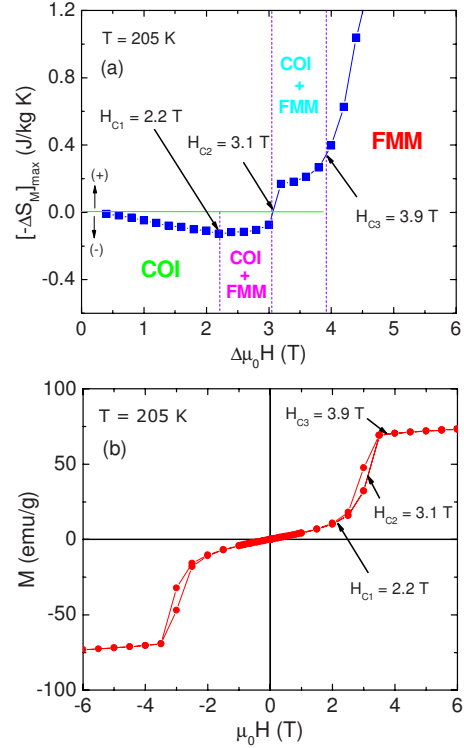


FIG. 5. (Color online) (a) Magnetic field dependence of maximum magnetic-entropy change ($-\Delta S_M^{\max}$) for LPCMO at 205 K; (b) the magnetic hysteresis loop $M(H)$ measured at 205 K. $H_{C1}=2.2$ T—the critical magnetic field at which the COI phase starts to convert into the FMM phase; $H_{C2}=3.1$ T—the critical magnetic field at which the half of the COI phase converts to the FMM phase; $H_{C3}=3.9$ T—the critical magnetic field at which the COI phase converts fully into the FMM phase. COI=charge-order insulator; FMM=ferromagnetic metal; the mixed phase range (both the COI and FMM phases coexist) is between H_{C1} and H_{C3} .

ing from the COI \rightarrow FMM conversion (~ 2.44 J/kg K). These findings clearly suggest that the sharp increase in the magnetization below T_C in LPCMO cannot be due to the destabilization of the COI phase^{11,12} but instead can be attributed to the enhancement of the pre-existing FMM domain regions.^{8,10,15,17} The hysteresis appearing below $H_{S2} \sim 2.6$ T is the result of the coexistence of the COI and FMM phases, whereas the application of higher fields ($H > 2.6$ T) completely suppresses the COI phase and as a result the FMM phase with no hysteresis is observed at these magnetic fields.

Finally, we note that the subtle balance between the competing COI and FMM phases in LPCMO is readily affected by applied magnetic field, and study of such a balance can be of great importance in elucidating the physical origin of magnetic/electric field-induced “colossal” effects.^{6,15,35-39} Here, we show that the change in magnitude and sign of $-\Delta S_M$ can be an indicator of the intricate balance between the COI and FMM phases as seen in the change in sign of $-\Delta S_M^{\max}$ at 205 K ($\sim T_{CO}$) as the applied magnetic field is increased. As shown in Fig. 5(a), the $-\Delta S_M^{\max}$ is *negative* and first increases in magnitude with increasing H up to $H_{C1} \sim 2.2$ T and then decreases and reaches zero at $H_{C2} \sim 3.1$ T. For $H > H_{C2}$, it is *positive* and increases gradu-

ally with increasing H up to $H_{C3} \sim 3.9$ T and finally increases rapidly for $H > H_{C3}$. Here $H_{C1}=2.2$ T is a critical magnetic field at which the COI phase starts to convert into the FMM phase, $H_{C2}=3.1$ T is a critical magnetic field at which the half of the COI phase converts into the FMM phase, and $H_{C3}=3.9$ T is a critical magnetic field at which the COI phase converts fully into the FMM phase.

The magnetic field dependence of $-\Delta S_M^{\max}$ can be interpreted as follows. For $H < H_{C1}$, the applied magnetic field is not strong enough to convert the COI phase into the FMM phase, so the negative $-\Delta S_M$ and its increase with H result from the contribution of the COI phase. However, for $H_{C1} < H < H_{C2}$, the positive contribution to $-\Delta S_M$ from the FMM phase becomes significant because the COI phase is partially converted into the FMM phase. Since the contribution from the FMM phase is opposite to that from the COI phase, the sum of the two components lead to a decrease in magnitude of the negative $-\Delta S_M$ with H in the range $H_{C1} < H < H_{C2}$. In other words, both the COI and FMM phases coexist but the COI phase is dominant over the FMM phase, since the sign of $-\Delta S_M$ is negative. At $H \sim H_{C2}$, the positive and negative contributions to $-\Delta S_M$ from the COI and FMM phases are equal or compensated and so $-\Delta S_M$ crosses zero. For $H_{C2} < H < H_{C3}$, the COI phase is largely converted into the FMM phase which now dominates over the COI phase leading to a positive $-\Delta S_M$. For $H > H_{C3}$, the COI phase is fully converted into the FMM phase leading to a rapid increase in magnitude of positive $-\Delta S_M$. The values of H_{C1} , H_{C2} , and H_{C3} coincide with the critical magnetic fields determined from the M - H curve [see Fig. 5(b)]. The hysteresis seen in the M - H curve between H_{C1} and H_{C3}

[Figs. 2(b) and 5(b)] is fully consistent with the coexistence of the COI and FMM phases as already revealed by the MCE data [Fig. 5(a)]. These results provide important understanding of the physical origin of the magnetic/electric field-induced “colossal” effects, including colossal magnetoresistance and large magnetocaloric effects in mixed-phased manganites.^{6,38,40,41}

In summary, systematic magnetocaloric measurements on $\text{La}_{5/8-y}\text{Pr}_y\text{Ca}_{3/8}\text{MnO}_3$ ($y=0.275$) single crystals have revealed further insights into the complex multiple-phase transitions. The system is ferromagnetic at low temperature and becomes charge ordered at high temperature. The dynamic strain-liquid phase is strongly affected by an applied magnetic field, whereas the frozen strain-glass phase is nearly magnetic field independent. The origin of the large MCE in the strain-liquid region arises from the suppression of dynamic fluctuations in magnetic fields. The MCE data clarify better that the sharp increase in the magnetization below T_C may not be due to the destabilization of the COI phase to the FMM phase, but favors the idea of the growth of pre-existing FMM domain regions. Overall, MCE is shown to be a very useful probe of the magnetic transitions and ground-state magnetic properties of mixed-phase systems.

ACKNOWLEDGMENTS

Work at USF was supported by the US Department of Energy through Grant No. DE-FG02-07ER46438. Work at Rutgers was supported by the US Department of Energy through Grant No. DE-FG02-07ER46382.

*Corresponding author.

[†]mphan@cas.usf.edu

[‡]sharihar@cas.usf.edu

¹Y. Tokura and Y. Tomioka, *J. Magn. Magn. Mater.* **200**, 1 (1999).

²*Colossal Magnetoresistance, Charge Ordering and Related Properties of Manganese Oxides*, edited by C. N. R. Rao and B. Raveau (World Scientific, Singapore, 1998); *Colossal Magnetoresistance Oxides*, edited by Y. Tokura, Monographs in Condensed Matter Science (Gordon and Breach, New York, 1999).

³Y. Tomioka, A. Asamitsu, Y. Moritomo, H. Kuwahara, and Y. Tokura, *Phys. Rev. Lett.* **74**, 5108 (1995).

⁴Y. Tomioka, A. Asamitsu, H. Kuwahara, Y. Moritomo, and Y. Tokura, *Phys. Rev. B* **53**, R1689 (1996).

⁵M. Tokunaga, N. Miura, Y. Tomioka, and Y. Tokura, *Phys. Rev. B* **57**, 5259 (1998).

⁶M. Uehara, S. Mori, C. H. Chen, and S.-W. Cheong, *Nature (London)* **399**, 560 (1999).

⁷K. H. Kim, M. Uehara, C. Hess, P. A. Sharma, and S.-W. Cheong, *Phys. Rev. Lett.* **84**, 2961 (2000).

⁸V. Kiryukhin, B. G. Kim, V. Podzorov, S.-W. Cheong, T. Y. Koo, J. P. Hill, I. Moon, and Y. H. Jeong, *Phys. Rev. B* **63**, 024420 (2000).

⁹I. G. Deac, S. V. Diaz, B. G. Kim, S.-W. Cheong, and P. Schiffer,

Phys. Rev. B **65**, 174426 (2002).

¹⁰H. J. Lee, K. H. Kim, M. W. Kim, T. W. Noh, B. G. Kim, T. Y. Koo, S.-W. Cheong, Y. J. Wang, and X. Wei, *Phys. Rev. B* **65**, 115118 (2002).

¹¹P. A. Sharma, S. B. Kim, T. Y. Koo, S. Guha, and S.-W. Cheong, *Phys. Rev. B* **71**, 224416 (2005).

¹²L. Ghivelder and F. Parisi, *Phys. Rev. B* **71**, 184425 (2005).

¹³W. Wu, C. Israel, N. Hur, S. Y. Park, S.-W. Cheong, and A. Lozanne, *Nature Mater.* **5**, 881 (2006).

¹⁴D. Gillaspie, J. X. Ma, H. Y. Zhai, T. Z. Ward, H. M. Christen, E. W. Plummer, and J. Shen, *J. Appl. Phys.* **99**, 08S901 (2006).

¹⁵T. Dhakal, J. Tosado, and A. Biswas, *Phys. Rev. B* **75**, 092404 (2007); S. H. Yun, T. Dhakal, D. Goswami, G. Singh, A. Herbad, and A. Biswas, *J. Appl. Phys.* **103**, 07E317 (2008).

¹⁶P. A. Sharma, S. El-Khatib, I. Mihut, J. B. Betts, A. Migliori, S. B. Kim, S. Guha, and S.-W. Cheong, *Phys. Rev. B* **78**, 134205 (2008).

¹⁷M. Kim, H. Barath, S. L. Cooper, P. Abbamonte, E. Fradkin, M. Rübhausen, C. L. Zhang, and S.-W. Cheong, *Phys. Rev. B* **77**, 134411 (2008).

¹⁸A. Moreo, M. Mayr, A. Feiguin, S. Yunoki, and E. Dagotto, *Phys. Rev. Lett.* **84**, 5568 (2000); E. Dagotto, *Science* **309**, 257 (2005).

¹⁹M. Uehara and S.-W. Cheong, *Europhys. Lett.* **52**, 674 (2000).

- ²⁰H. Kuwahara, Y. Tomioka, A. Asamitsu, Y. Moritomo, and Y. Tokura, *Science* **270**, 961 (1995).
- ²¹M. H. Phan and S. C. Yu, *J. Magn. Magn. Mater.* **308**, 325 (2007).
- ²²M. S. Reis, V. S. Amaral, J. P. Araujo, P. B. Tavares, A. M. Gomes, and I. S. Oliveira, *Phys. Rev. B* **71**, 144413 (2005).
- ²³A. Biswas, T. Samanta, S. Banerjee, and I. Das, *Appl. Phys. Lett.* **92**, 012502 (2008).
- ²⁴M. H. Phan, N. A. Frey, M. Angst, J. de Groot, B. C. Sales, D. G. Mandrus, and H. Srikanth, *Solid State Commun.* **150**, 341 (2010).
- ²⁵M. H. Phan, G. T. Woods, A. Chaturvedi, S. Stefanoski, G. S. Nolas, and H. Srikanth, *Appl. Phys. Lett.* **93**, 252505 (2008).
- ²⁶P. Sande, L. E. Hueso, D. R. Miguens, J. Rivas, F. Rivadulla, and M. A. Lopez-Quintela, *Appl. Phys. Lett.* **79**, 2040 (2001).
- ²⁷P. J. von Ranke, N. A. de Oliveira, B. P. Alho, E. J. R. Plaza, V. S. R. de Sousa, L. Caron, and M. S. Reis, *J. Phys.: Condens. Matter* **21**, 056004 (2009).
- ²⁸A. Giguere, M. Foldeaki, B. Ravi Gopal, R. Chahine, T. K. Bose, A. Frydman, and J. A. Barclay, *Phys. Rev. Lett.* **83**, 2262 (1999).
- ²⁹H. Wada and Y. Tanabe, *Appl. Phys. Lett.* **79**, 3302 (2001).
- ³⁰G. J. Liu, J. R. Sun, J. Shen, B. Gao, H. W. Zhang, F. X. Hu, and B. G. Shen, *Appl. Phys. Lett.* **90**, 032507 (2007).
- ³¹N. S. Bingham, M. H. Phan, H. Srikanth, M. A. Torija, and C. Leighton, *J. Appl. Phys.* **106**, 023909 (2009).
- ³²J. S. Amaral and V. S. Amaral, *Appl. Phys. Lett.* **94**, 042506 (2009).
- ³³J. D. Moore, G. K. Perkins, K. Morrison, L. Ghivelder, M. K. Chattopadhyay, S. B. Roy, P. Chaddah, K. A. Gschneidner, Jr., V. K. Pecharsky, and L. F. Cohen, *J. Phys.: Condens. Matter* **20**, 465212 (2008).
- ³⁴N. A. de Oliveira, P. J. von Ranke, M. V. Tovar Costa, and A. Troper, *Phys. Rev. B* **66**, 094402 (2002).
- ³⁵G. Garbarino, M. Monteverde, C. Acha, P. Levy, M. Quintero, T. Y. Koo, and S.-W. Cheong, *Physica B* **354**, 16 (2004).
- ³⁶P. Levy, F. Parisi, M. Quintero, L. Granja, J. Curiale, J. Sacanell, G. Leyva, G. Polla, R. S. Freitas, and L. Ghivelder, *Phys. Rev. B* **65**, 140401(R) (2002).
- ³⁷H. T. Yi, T. Choi, and S. W. Cheong, *Appl. Phys. Lett.* **95**, 063509 (2009).
- ³⁸J. Tosado, T. Dhakal, and A. Biswas, *J. Phys.: Condens. Matter* **21**, 192203 (2009).
- ³⁹G. Singh-Bhalla, S. Selcuk, T. Dhakal, A. Biswas, and A. F. Hebard, *Phys. Rev. Lett.* **102**, 077205 (2009).
- ⁴⁰L. Ghivelder, R. S. Freitas, M. G. das Virgens, H. Martinho, L. Granja, G. Leyva, P. Levy, and F. Parisi, *Phys. Rev. B* **69**, 214414 (2004).
- ⁴¹A. L. Lima Sharma, P. A. Sharma, S. K. McCall, S.-B. Kim, and S.-W. Cheong, *Appl. Phys. Lett.* **95**, 092506 (2009).